

## In Vivo Modulation of Hippocampal Epileptiform Activity with Radial Electric Fields

\*†Kristen A. Richardson, \*†Bruce J. Gluckman, ‡Steven L. Weinstein, \*Caryn E. Glosch,  
\*Jessica B. Moon, §Ryder P. Gwinn, ||Karen Gale, and \*¶Steven J. Schiff

\*Krasnow Institute, and †Department of Physics and Astronomy, George Mason University, Fairfax, Virginia; ‡Department of Neurology, Children's National Medical Center and George Washington University School of Medicine; and Departments of §Neurosurgery and ||Pharmacology, Georgetown University, Washington, D.C.; and ¶Department of Psychology, George Mason University, Fairfax, Virginia, U.S.A.

**Summary:** *Purpose:* Electric field stimulation can interact with brain activity in a subthreshold manner. Electric fields have been previously adaptively applied to control seizures in vitro. We report the first results from establishing suitable electrode geometries and trajectories, as well as stimulation and recording electronics, to apply this technology in vivo.

*Methods:* Electric field stimulation was performed in a rat kainic acid injection seizure model. Radial electric fields were generated unilaterally in hippocampus from an axial depth electrode. Both sinusoidal and multiphasic stimuli were applied. Hippocampal activity was recorded bilaterally from tungsten microelectrode pairs. Histologic examination was performed to establish electrode trajectory and characterize lesioning.

*Results:* Electric field modulation of epileptiform neural activity in phase with the stimulus was observed in five of six si-

nusoidal and six of six multiphasic waveform experiments. Both excitatory and suppressive modulation were observed in the two experiments with stimulation electrodes most centrally placed within the hippocampus. Distinctive modulation was observed in the period preceding seizure-onset detection in two of six experiments. Short-term histologic tissue damage was observed in one of six experiments associated with high unbalanced charge delivery.

*Conclusions:* We demonstrated in vivo electric field modulation of epileptiform hippocampal activity, suggesting that electric field control of in vivo seizures may be technically feasible. The response to stimulation before seizure could be useful for triggering control systems, and may be a novel approach to define a pre-seizure state. **Key Words:** Electric field—Neural prosthesis—Seizure—Hippocampus—Preseizure state—Epilepsy.

Although control system technology has made extraordinary advances during the past century, our efforts to apply sophisticated control strategies to epilepsy have been limited. Such limitations arise both from the lack of a flexible control parameter that would permit us to increase or decrease activity in the brain rapidly and reversibly, and the lack of stimulation and recording amplifiers designed for simultaneous monitoring of neuronal activity during control stimulation. Uninterrupted monitoring would allow a control system to use ongoing information about the dynamics to prescribe the control perturbations as continuous feedback. The application of continuous feedback would allow a controller to modify spe-

cific patterns of neuronal activity selectively while minimizing the impact on other more normal activities. This approach is in contrast to “reversible lesions” associated with high-frequency stimulation, which more indiscriminately suppresses neuronal activity in the neighborhood of stimulation. We here demonstrate in vivo some technical solutions required for future implementation of continuous feedback control of seizures by using electric field stimulation.

Early strategies for controlling epileptic seizures through electrical stimulation focused on stimulating sites in the brain distant from the presumed epileptic focus. Such indirect stimulation made use of the cerebellum, but initially encouraging reports (1) were difficult to replicate (2). Favorable reports of stimulation of the centromedian nucleus of the thalamus (3,4) were difficult to replicate in a controlled setting (5), and a recent controlled trial failed to demonstrate a return to baseline seizure frequency after stimulation (6). Anecdotal reports of stimulation of the subthalamic nucleus for epilepsy have been reported

Accepted January 19, 2003.

Address correspondence and reprint requests to Dr. B.J. Gluckman at Department of Physics and Astronomy and the Krasnow Institute, George Mason University, Fairfax, VA 22030-4444, U.S.A. E-mail: BGluckma@gmu.edu

Doctors Richardson and Gluckman contributed equally to first authorship.

(7–9). A recent report (10) of prolonged anterior thalamic stimulation failed to demonstrate an additional decrease in seizure rate after stimulation was initiated compared with the postoperative effects of electrode insertion. Further deep-brain structures that are candidates for indirect stimulation are being explored in laboratory settings (11,12).

Another indirect stimulation strategy has been directed at stimulation of cranial nerves, especially the vagus (13). The efficacy of this technique in long-term studies falls short of the expectations for resective treatment (14,15), and recently the physiological foundation for this technique has been questioned (16). Alternative cranial nerves for stimulation are being explored in laboratory settings (17,18).

Developing the technical capability for direct interaction with an epileptic focus has been an attractive subject for both laboratory and clinical investigation. As a medical therapy, direct interaction offers the prospect of a highly targeted treatment that, through spatial confinement, would limit side effects. Various laboratory studies have investigated focal drug-delivery systems (19,20), and recently focal cooling (21,22).

A growing body of experimental data also examined the prospect of direct electrical stimulation to suppress seizures. In the *in vitro* slice experiments, stimulation was shown to inhibit seizure formation in a manner similar to the effects of interictal burst firing activity (23,24), and the low-frequency range that will produce this effect seems narrow (25). Reports of *in vivo* prolonged poststimulus suppressive effects of low-frequency pulsatile stimulation (26) were found related to low-level direct current (DC) leakage and may have been associated with tissue damage (27).

Several reports described direct stimulation of human epileptic foci *in vivo*. Continuous stimulation over a 2- to 3-week period appeared to suppress seizures (28), and an uncontrolled report of long-term hippocampal stimulation showed similar results (29). Most recently, trains of pulse stimulation were found to suppress afterdischarges during cortical mapping (30,31).

All of these efforts used traditional pulse stimulation, usually with charge-balanced biphasic waveforms with short (millisecond) duration. Such stimulation clearly interacts with ongoing neural activity, and well-established safety guidelines are available for such stimuli (32,33). Although individual bipolar pulses may generate time-locked impulses of action potentials, recent experimental work suggests that trains of sustained large-amplitude stimuli induce depolarization block of neuronal activity (34). The large instantaneous electric currents and potentials associated with pulsatile stimuli generally preclude simultaneous monitoring of neural activity, so that continuous feedback based on the epileptic brain activity is not possible.

We have been investigating the prospect of using continuous electric fields and currents to modulate epileptic activity. In contrast to pulsatile stimulation, continuous electric field stimulation provides a means for either excitatory or suppressive modulation of ongoing neural activity depending on field sign, and the response is graded with respect to field amplitude. Importantly, electric fields can be applied without interfering with simultaneous monitoring of neural activity. In principle, control systems based on continuous electric field stimulation would supply only the current needed to modify a pathologic neuronal activity and thereby minimize risk of tissue damage and minimize impact on other behaviors.

A long history of using polarized electric fields or currents to modulate neural activity is known (see, for example, 35–37), and the mechanism for electric field modulation is well understood (38–41). Small electric fields polarize neurons with long asymmetric dendritic trees, shifting their somatic transmembrane potentials and making the neurons either closer to or further from threshold for action potential initiation. The magnitude and sign of the polarization is proportional to the field amplitude and sign. In contrast to pulse stimulation, electric fields can therefore be applied in a true subthreshold fashion, biasing up or down the response of neurons to their native inputs.

In earlier work, we demonstrated that small DC fields could reversibly modulate interictal activity in a graded fashion and suppress or excite epileptiform events (42). Ghai et al. (43) demonstrated that not only were electrographic epileptiform events suppressed with DC field application, but that the associated variations in extracellular potassium during such events were also suppressed. We recently showed that electric fields applied adaptively in a feedback loop incorporating simultaneous monitoring of neural activity can control *in vitro* seizure-like events (44). We here report the first results from establishing suitable electrode geometries and trajectories, as well as stimulation and recording electronics, required to translate these *in vitro* results to *in vivo* use.

## METHODS

This work was performed in accordance with National Institutes of Health (NIH) vertebrate animal guidelines with approval of the George Mason University Animal Care and Use Committee.

### Materials and electronics

#### *Surgical procedures*

Male Sprague–Dawley rats (average, 284 g; 65 days old) were anesthetized with a ketamine/xylazine (KX) mixture of 100 mg/ml ketamine with 20 mg/ml xylazine in a ratio of 8:1 by volume, administered in doses of 0.1 ml/100 g. Once the animal was areflexive (determined

by toe or tail pinch), it was stabilized with ear and incisor bars. Additional doses of KX were administered throughout the experiment to maintain areflexia. Core temperature was monitored with a rectal thermometer and controlled with a heating pad. A vertex incision was made to expose the skull from the anterior frontal bone to the external occipital crest. A 4-mm-wide craniotomy was performed bilaterally from the coronal to the lambdoid sutures, leaving a 2-mm strip of bone over the sagittal sinus intact. The dura mater covering the left hemisphere was opened, exposing the neocortex. A left neocortical window was created with aspiration to enter the body of the lateral ventricle and expose the dorsal surface of the hippocampus. On the right, a small opening was created in the center of the dura for stereotactic electrode insertion. Both exposed brain areas were kept moist with a layer of artificial cerebrospinal fluid (aCSF) containing (in mM): 155 Na<sup>+</sup>, 136 Cl<sup>-</sup>, 3.5 K<sup>+</sup>, 1.2 Ca<sup>2+</sup>, 1.2 Mg<sup>2+</sup>, 1.25 PO<sub>4</sub><sup>2-</sup>, 24 HCO<sub>3</sub><sup>-</sup>, 1.2 SO<sub>4</sub><sup>2-</sup>, and 10 dextrose.

#### Recording electronics

Field potential recordings were made from differential microelectrode pairs (tungsten, 3 MΩ impedance, fixed

240-μm spacing; Frederic Haer Corporation). Two electrode pairs were inserted into the body of the left hippocampus to a depth of ~0.2 mm. A third recording electrode was stereotactically inserted through the right neocortex into the body of the right hippocampus. An additional agar bridge electrode placed in contact with the aCSF fluid layer in the left cortical window served as measurement ground. A photograph and schematic of electrode placements are shown in Fig. 1. Signals from the microelectrode pairs were differentially preamplified with custom-built headstages (gain 10), and then conditioned by using a standard amplifier bank (EX4-400; Dagan Corporation) with additional gains of 20–100 and bandpass filtered with high-pass frequency of 3–5 Hz and low-pass of 3 kHz. Each signal was then digitally recorded by using Axon Instruments hardware and software (12 bits/sample, 5 kHz; DigiData 1200a, Axoscope).

Field potentials were recorded differentially by using closely spaced electrode pairs to minimize the effect of the applied electric field. The custom differential preamplifiers (based on instrumentation amplifiers Analog Devices AMP02 or Texas Instrument INA116) accommodated common-mode signals between the recording

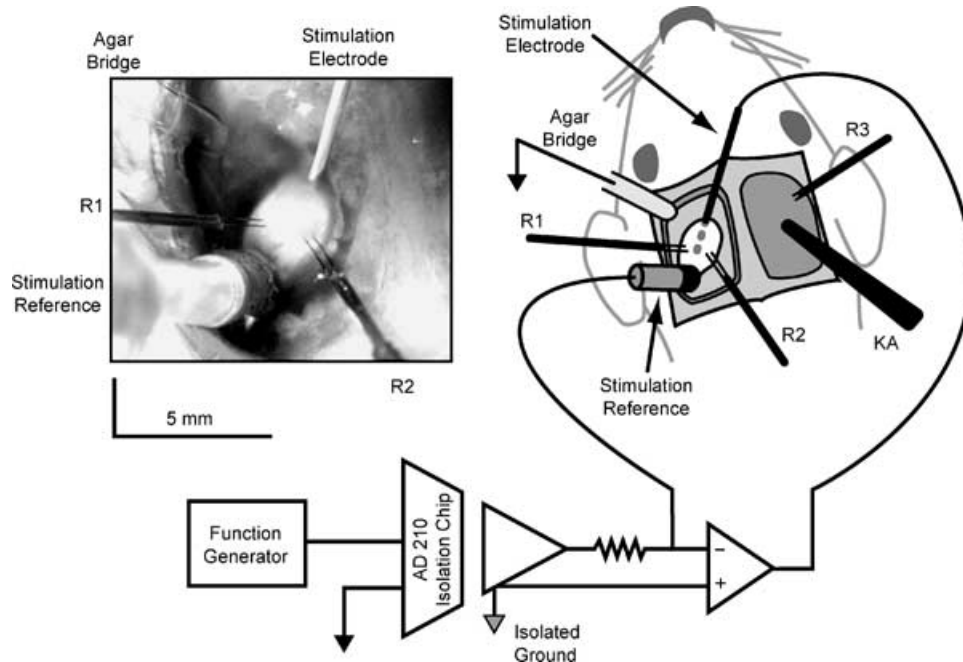


**FIG. 1.** Photo of left hippocampus and hardware during experiment 4, and schematic of experimental preparation and stimulation electronics. Two recording microelectrode pairs (R1 and R2) were inserted into the body of the exposed left hippocampus. A third recording microelectrode pair (R3) was inserted through the intact right neocortex into the right hippocampus. An agar bridge placed in contact with the artificial cerebrospinal fluid (aCSF) fluid layer over the rostral portion of the left cortical cavity served as measurement ground. An injection cannula (kainic acid; KA) for the perfusion of KA into the right hippocampus was inserted vertically into the CA1 through a dural window. The stimulation electrode was inserted along the center axis of the exposed left hippocampus, whereas the stimulation reference plate was placed in the aCSF fluid layer in the lateral posterior region of the left neocortical window. The stimulation current was created by a voltage-to-current amplifier with transformer-coupled isolation of both input and power (with an Analog Devices AD210) programmed from a standard waveform generator.

electrodes and measurement ground produced by the applied electric field.

#### Stimulation electrodes and electronics

A large-scale electric field was applied by driving current between two electrodes in electrical contact with the tissue. A rod-shaped depth electrode (Ag-AgCl, 0.25-mm diameter) was inserted along the central axis of the left hippocampus to a depth of  $\sim 3$  mm and referenced to a circular plate electrode (2-mm diameter Ag-AgCl) placed in the aCSF layer near the left hippocampus within the cortical window. The electric field from such an axially placed cylindrical electrode is approximately radial, falls off inversely proportional to the distance from the long axis, and modulates large regions of CA3, CA2, and CA1 pyramidal neurons. An analytic approximation of the field, based on a uniform tissue conductivity of  $125 \Omega\text{cm}$  (45), is illustrated in Fig. 2.

The stimulation current was created by a voltage-to-current amplifier with transformer-coupled isolation of

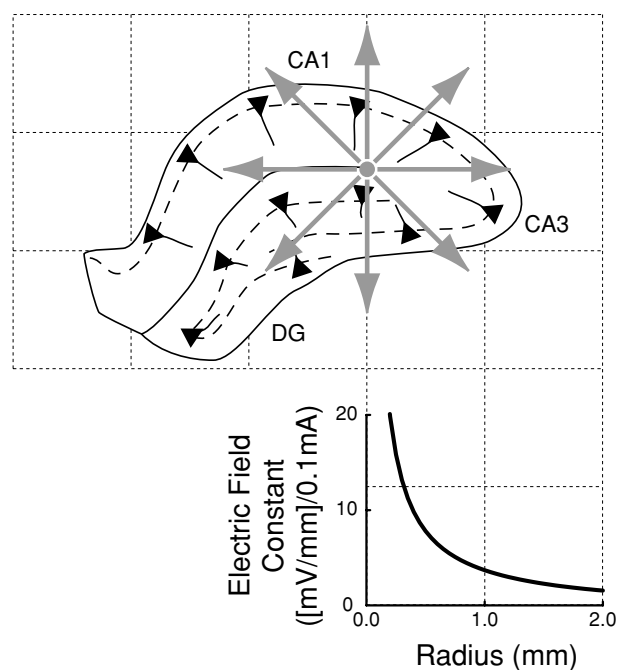


**FIG. 2.** Electric field geometry and amplitude for depth electrode placed axially within hippocampus. For fixed stimulation electrodes, the geometry of the electric field is constant, whereas the amplitude of the field will be linearly proportional to the current applied between stimulation electrodes. **Top:** Illustration of geometry of field within perpendicular midplane of electrode from analytic calculation. The field is radial, and parallel to the long dendrite–soma axis of the pyramidal neurons in large regions of both CA3 and CA1. **Bottom:** Proportionality constant between field and applied current, based on depth electrodes used (0.25 mm diameter, 5 mm long) and uniform tissue conductivity of  $125 \Omega\text{cm}$  (45). Along the perpendicular midplane, the field should fall off proportional to  $\frac{1}{r\sqrt{1+4(r/l)^2}}$  (solution for a finite length line source), where  $r$  is the radius and  $l$  is the length of the electrode.

both input and power (with an Analog Devices AD210). This allows the stimulation electrode potentials to float with respect to the measurement “ground.” Control signals were produced with a waveform generator (Hewlett Packard 33120A). The stimulation electronics are shown schematically in Fig. 1.

#### Experimental protocol

##### Overview

A 0.25-mm (o.d.) cannula for the injection of kainic acid (KA; OPIKA-1 Kainic Acid, Ocean Produce International) was inserted stereotactically into the right hippocampal CA1 (5.6 mm posterior to bregma, 4.5 mm lateral, and 3.0 mm deep to the cortical surface) through the dural window and intact cortex. A microperfusion pump was used to introduce  $0.55 \mu\text{l}$  of  $200 \text{ ng}/\mu\text{l}$  KA into the hippocampus, repeated if needed at 20-min intervals (one to six applications) until epileptiform activity was observed. In one experiment, placing the KA-loaded cannula into the CA1 was sufficient to provoke epileptiform activity, and no bolus injections were administered. After the experiments, animals were euthanized with an overdose of anesthesia (0.4–0.6 ml KX).

##### Electric field stimulation

Electric field stimulation was applied with either sinusoidal or multiphase square-waves (phasic) with varying amplitudes and periods. The phasic waveform was constructed with consecutive plateaus of amplitude  $[0, 1, 0, -1]$ , each of equal duration (see Fig. 3) and connected smoothly to minimize frequency components  $>25$  times the waveform frequency. Afterward, other continuous waveforms, notably long DC pulses, also were applied for exploratory purposes.

##### Analysis

Averages values are presented as mean  $\pm$  standard deviation.

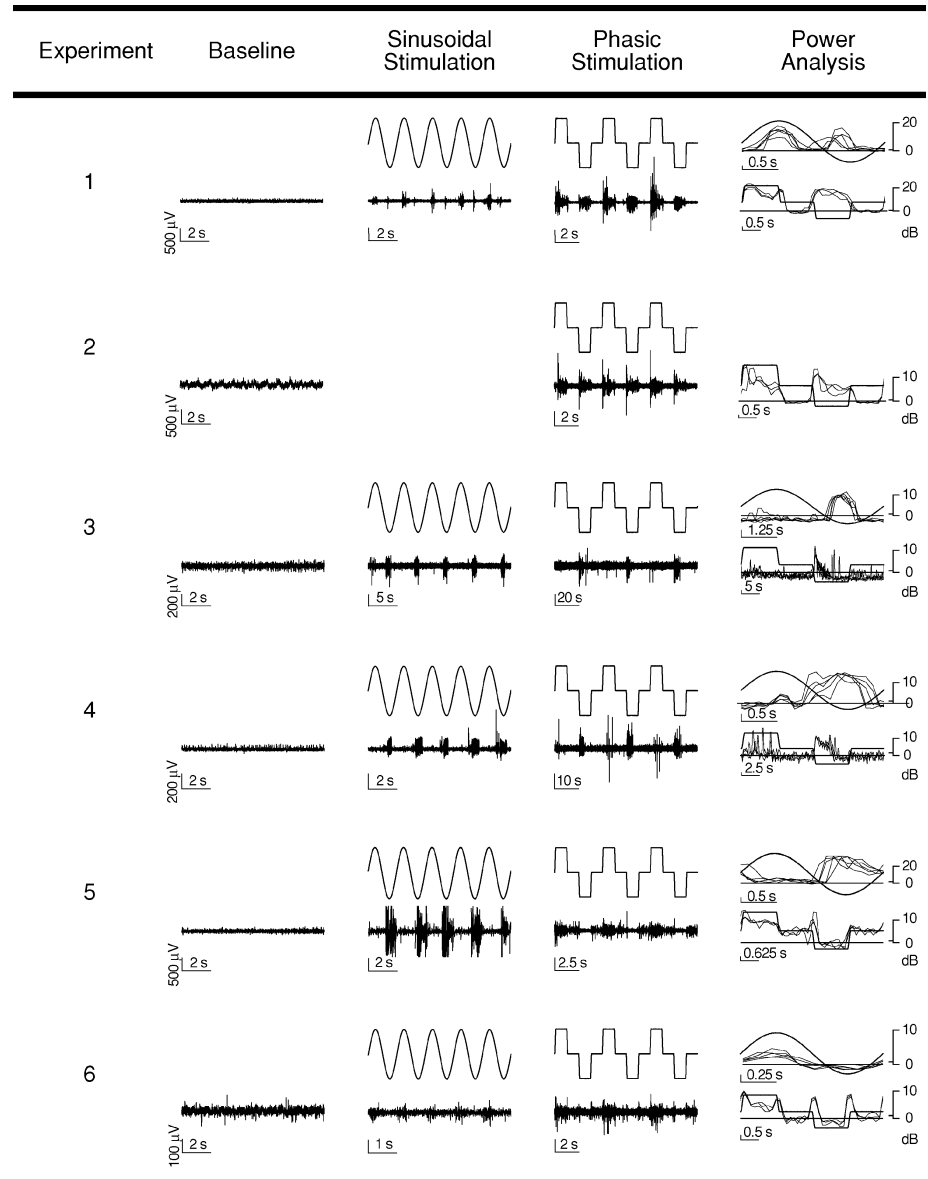
##### Peristimulus RMS

Recordings (baseline and during stimulation) were digitally bandpass filtered with a second-order Chebyshev filter (high-pass, 10–20 Hz; low-pass, 2 kHz) to remove residual stimulus artifact. We quantified the degree of modulation with the root mean squared (RMS) power in the pass band from the field-potential recordings. The average RMS is calculated in half overlapping 200-ms windows.

##### RMS per phase

For the phasic stimuli, the RMS activity,  $\sigma$ , was calculated for each phase of the stimulus for measurements in both the stimulated and the KA hippocampus (electrodes R1 and R3, respectively). Further to quantify the modulation of activity by the electric field as the

**FIG. 3.** Modulation of hippocampal field potential activity by sinusoidal and phasic radial electric field stimulation from six experiments. Traces: Field potential traces were measured from the stimulated hippocampus during baseline activity and during sinusoidal and multiphasic electrical stimulation. Calibration bars indicate field potential amplitude in microvolts (vertical) and time in seconds (horizontal). Amplitude and frequency of the stimuli and measurement electrode identification are listed in Table 1. The sinusoidally stimulated response trace from experiment 5 was vertically clipped for presentation. Sinusoidal and phasic response data were bandpass filtered (10–20 Hz to 2 kHz) to reduce stimulation artifact. Power analysis: Power was calculated from 200-ms half-overlapped windows with phase of stimuli overlaid, and plotted in decibels (dB) relative to average baseline power [ $dB = 20 \log(RMS/RMS_{baseline})$ ] for each period of stimulus shown in the traces. One standard deviation of window-to-window baseline power fluctuation is indicated by left-heading hashmark (-) along vertical axes and can be used as an estimate of significance for observed fluctuations. One period of the stimulus is overlaid as a visual guide.



ongoing activity changes, the normalized RMS deviation  $\Delta = (\sigma - \bar{\sigma}_z) / \bar{\sigma}_z$ , was calculated, where  $\sigma$  is the RMS activity averaged over either the positive or the negative phase of the stimulus, and  $\bar{\sigma}_z$  is the RMS activity averaged over the previous and subsequent zero-amplitude phases of the stimulus.

#### Seizure-onset times

Seizure-onset times were defined when  $\sigma$  for all stimulation phases on the KA side (electrode R3) exceeded threshold for 2 s. The threshold was chosen at a convenient value that eliminated false positives. We found that it was possible to define a pre-seizure onset time when  $\sigma$  exceeded the same threshold for just one phase of the phasic waveform over at least two waveform periods.

#### Histology

After euthanization, the brain was removed intact and fixed in 4% paraformaldehyde, and then sectioned and stained with hematoxylin and eosin (H&E) to establish electrode placement and examine the tissue histologically. Basic histologic analysis was performed to determine the stimulation-electrode trajectory and screen for evidence of acute damage to the tissue. In each of the histologic slices, the position of the electrode track was identified by local tissue disruption. This position was then sketched along with gross anatomic structure and major cell body layers and mapped onto reference images derived from the Paxinos and Watson rat brain atlas (46). Reconstructed electrode positions in intermediate reference images were then plotted by linear interpolation.

RESULTS

Interictal modulation

Electrical field modulation of ongoing hippocampal activity from the stimulated hippocampus is shown in Fig. 3, with examples of the different stimuli and typical responses for each of the six experiments. Baseline traces represent activity in each experiment either immediately before or after electrical field application. Stimuli characteristics and recording electrode identification for this figure are summarized in Table 1.

Peristimulus RMS activity for each period of sinusoidal or phasic stimulus in the traces is shown in the power analysis. Vertical axes at the right are RMS power in dB referenced to the average RMS power calculated in 200-ms windows from 10 s of baseline data recorded near in time to each stimulation protocol. The standard deviation (STD) of the average baseline RMS  $STD_{baseline}$  power is marked with a left-heading hash mark (-) on the power axes, and can be used as guide to estimate significance of the variations observed during stimulation. In each case, the maximum per period variation observed during stimulation is many times the baseline STD. This normalized deviation  $(RMS_{max} - RMS_{baseline})/STD_{baseline}$ , averaged over experiments, is  $60 \pm 14$  for sinusoidal and  $136 \pm 55$  for phasic stimuli.

In five of six experiments, RMS analysis revealed significant increase of activity at the positive and/or negative phase of the sinusoidal field. The neural response to particular phases of stimulation varied between experiments. In experiment 1 (row 1, Fig. 3), we observed an increase in activity and RMS at both the positive and negative phases of the sinusoid. Stimulus artifact from experiment 2 could not be successfully removed from the recordings, so results were indeterminate. In experiments 3 through 6, excitation of the ongoing neural activity occurred at a single phase of the stimulation.

Similar results are seen for the phasic stimulation. Excitation occurs at both the positive and negative phases of stimulation in experiments 1, 2, and 4. Experiment 3 demonstrated excitation almost exclusively on the nega-

tive phase of stimulation. The last two experiments, 5 and 6, demonstrated both excitation on the positive phase of stimulation and suppression of activity on the negative phase of the stimulation. This is quantified for a longer period from experiment 5 (Fig. 4).

Modulation before seizure onset

In two experiments (1 and 5), we observed characteristic changes in the neuronal response to stimulation in advance of the electrographic seizures.

An example from experiment 5 of bilateral activity modulation is shown in Fig. 4 for 25 min of phasic electric field stimulation (period, 2 s; amplitudes, 0.29, 0.33 and 0.50 mA). We calculated the RMS activity per phase,  $\sigma$ , for each 0.5-s phase of the stimulus for measurements in both the stimulated and the KA hippocampus (electrodes R1 and R3, respectively). Plotted in Fig. 4A is  $\sigma$  for recordings in each hippocampus, with stimulus phase color encoded (color code illustrated in boxed inset). Ipsilateral to the stimulation (Stim, lower graph), the positive phase (red) yielded higher  $\sigma$  than either zero phase (black and green), each of which was higher than the negative phase (blue).

This pattern is intermittently interrupted by periods with increased RMS that correspond to seizures. Electrographic seizure-onset times, defined when  $\sigma$  exceeded a threshold (gray line) for 2 s (four consecutive phases), are indicated with red arrows.

A bilateral recording of a single seizure is shown in Fig. 4B. Many seconds in advance of seizure-onset time, bursts of activity are observed contralateral to the stimulus starting at  $\sim 350$  s (upper trace). These bursts occur only on the *negative* phase of the stimulus, when the stimulated hippocampus was *suppressed*. Preseizure times defined when the activity on the KA side exceeded the same threshold as before (gray line) for two consecutive stimulus periods but only during the negative phase of the stimulus are shown with blue arrows. This preseizure-onset time preceded the full onset time (red arrows) by 17 s in this example.

Further to quantify the modulation of activity by the electric field as the ongoing activity changes, we introduce the normalized RMS deviation  $\Delta = (\sigma - \bar{\sigma}_z)/\bar{\sigma}_z$ , where  $\sigma$  is the RMS activity averaged over either the positive or negative phase of the stimulus, and  $\bar{\sigma}_z$  is the RMS activity averaged over the previous and subsequent zero-amplitude phases of the stimulus. Excitatory modulation appears as a positive  $\Delta$  and suppressive modulation as negative  $\Delta$ . The normalized RMS deviation is shown in Fig. 4C for the same data as in Fig. 4B. On the KA side, the negative phases, shown in blue, yield a positive  $\Delta$  just before the seizure onsets. This increase in activity on the KA side was repeated before each of the seven seizures observed in the 25 min of recording, shown in Fig. 4D. Preseizure-onset times as defined earlier (blue arrows) precede full

TABLE 1. Characteristics for traces and stimuli presented in Figure 3

Experiment	Recording electrode	Sinusoidal		Phasic stimulation	
		Amplitude (mA)	Frequency (Hz)	Amplitude (mA)	Frequency (Hz)
1	R2	0.25	0.5	1.0	0.25
2	R1	—	—	0.1	0.25
3	R2	1.25	0.2	1.2	0.025
4	R2	1.0	0.5	1.2	0.05
5	R1	0.37	0.5	0.3	0.2
6	R1	0.05	1.0	0.01	0.25

Traces presented were measured by using electrodes R1 or R2, as shown in Fig. 1. Amplitudes are peak-zero.

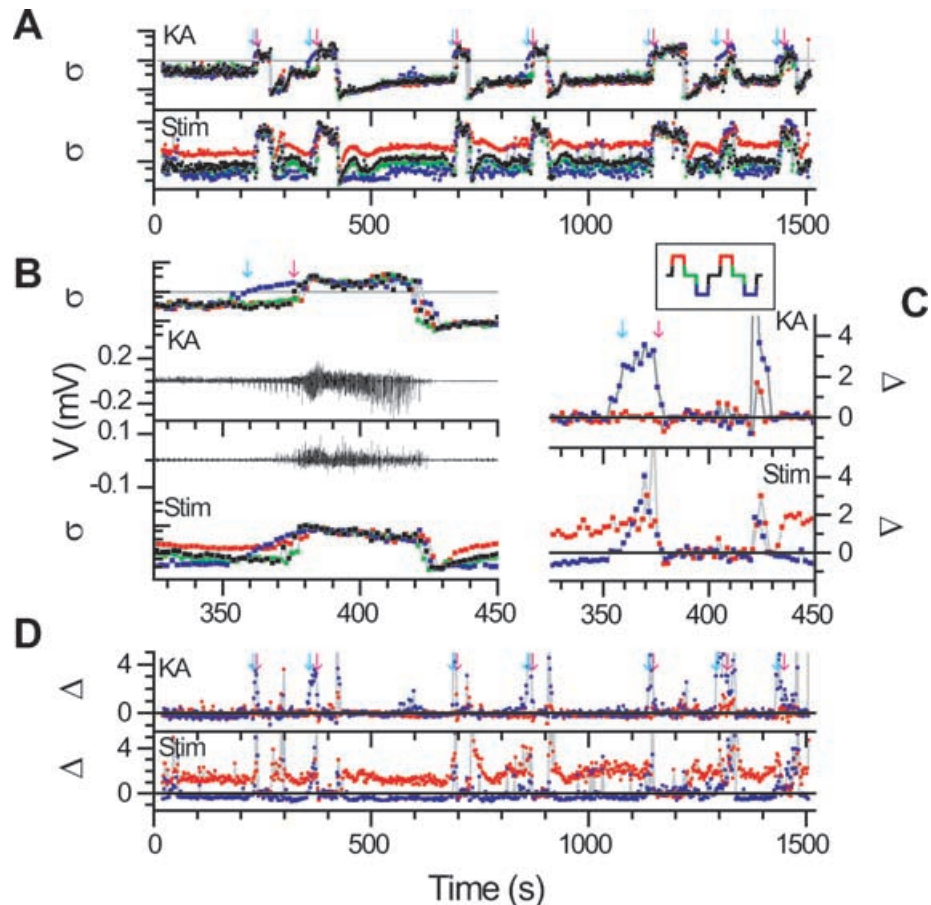


**FIG. 4.** Bilateral modulation between and during seizures. (Experiment 5: phasic stimulus, 2-Hz period; amplitudes, 0.29 mA  $0 < t < 225$  s, 0.33 mA  $225 < t < 685$  s, 0.50 mA  $685 < t < 1,500$  s). In each panel, the lower graphs correspond to measurements or analysis from the stimulated left hippocampus (*Stim*), and the upper graphs correspond to the right hippocampus that received the kainic acid injection (KA). **A:** Root mean square (RMS) activity per phase,  $\sigma$ , during a 25-min recording. Phase is color coded [(1, 0, -1, 0): (red, green, blue, black)] as illustrated in inset above **C**. Interictally,  $\sigma$  for the stimulated hippocampus (**lower graph**) is typically higher during the positive phase of the stimulus (*red*) and lowest during the negative phase (*blue*). This pattern is violated during seizures. **B:** Field potential traces and  $\sigma$  through the seizure at  $t = 375$  s. Vertical tick marks on traces correspond to 2-mV field-potential deflections. Significant excitatory responses on the KA side (**upper graphs**) are observed during the *negative* phase (*blue*) of the stimulus before the beginning of the seizure. **C:** Normalized RMS deviation  $\Delta = (\sigma - \bar{\sigma}_z) / \bar{\sigma}_z$  during the positive (*red*) and negative (*blue*) phases of the stimulus for the same period as in **B**. Contralateral to the stimulus (KA side),  $\Delta$  increased dramatically before the seizure. **D:**  $\Delta$  for the same period as in **A**. Contralateral to the stimulus (KA side),  $\Delta$  increased for the negative phase at the beginning of each seizure. Seizure-onset times (*red arrows*) defined when  $\sigma$  exceeded the threshold (*gray line*) for all stimulus phases on the KA side for  $\geq 2$  s. Preseizure onset times (*blue arrows*) defined when  $\sigma$  exceeded the threshold (*gray line*) for two consecutive stimuli periods only during the negative-stimulus phase. Preseizure-onset times precede seizure-onset times by  $14 \pm 2$  s for the seven seizures observed.

seizure-onset times (red arrows) by  $14 \pm 2$  s averaged over the seven seizures observed in the 25 min of this recording.

### Histology

Basic histologic analysis was performed to determine the stimulation electrode trajectory and screen for evidence of acute damage to the tissue. Images of histologic sections chosen from the anterior and posterior ends of the electrode track are shown for each experiment in Fig. 5A.

Reconstruction of the electrode track was possible for five of six experiments. In experiment 2, the electrode track could not be determined from the histologic sections,

preventing trajectory reconstruction. For experiments 1, 3, and 4, the electrode trajectory was steep and passed through the lower portion of the hippocampus. In experiments 3 and 4, it exited the ventral surface of the hippocampus.

The reconstructed electrode trajectories for experiments 5 and 6 are shown in Fig. 5B. The tracks remain within the center of the hippocampus. The insertion path at the dorsal surface of the hippocampus in the CA1 region was observed in slices just anterior to the portion illustrated; trajectory positions measured in more posterior slices remained at the upper surface of the dentate gyrus. Because of the central placement of the stimulation

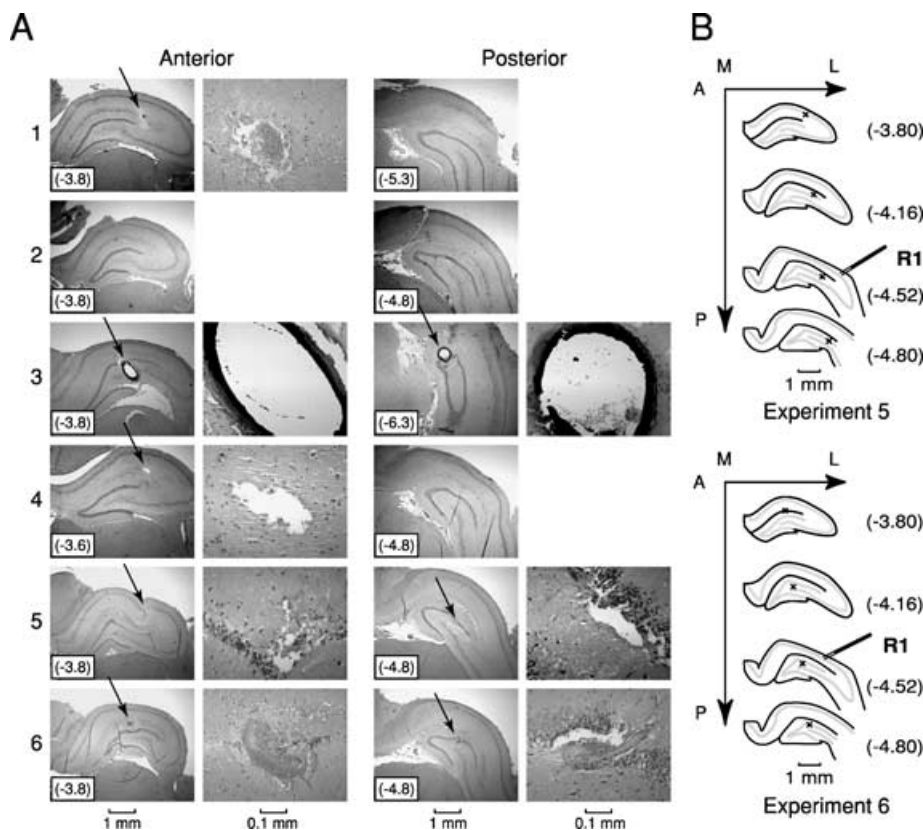


**FIG. 5.** Histologic images and stimulation electrode track reconstruction. **A:** Images from the anterior and posterior ends of the electrode trajectory for each experiment (numbered to the left), with magnified images of the electrode track shown when clearly visible (arrows). Approximate stereotaxic coordinates determined by comparison to a rat brain atlas (46). **B:** Electrode path reconstruction for experiments 5 and 6. The interpolated electrode trajectory for each is indicated on the atlas reference slices with an (x). The position of recording electrode R1 is estimated by cross-referencing surface photos from the experiment with the histologic sections and the rat atlas reference. Orientational notation: L, lateral; M, medial; A, anterior; P, posterior. Reproduced from reference 46, with permission.

electrode in these experiments, the electric field produced was aligned as shown in Fig. 2 for a significant length of the hippocampus. These two experiments demonstrated modulation of neuronal activity proportional to the amplitude of the applied field, with positive applied field yielding excitation and negative applied field yielding suppression (Fig. 3).

In five of six experiments, no evidence of lesioning beyond insertion damage was identified. However, in experiment 3, significant lesioning and Ag-AgCl deposition were observed along the electrode track. Tissue damage from electrodes and electrical stimulation can result from a number of mechanisms, the most common of which depends on polarization of the electrode/fluid interface, which is a function of the unbalanced charge passed (see Table 2 for details). When the potential across this interface exceeds the oxidation/reduction (redox) thresholds for various electrolytic reactions, reaction products are created that cause lesioning (see, for example, 47). Table 2 lists the statistics of charge passage for the different experiments. The maximum unbalanced charge in experiment 3 was 6 times the maximum charge passed in any other experiment. The large excursions in charge passage correspond to exploratory waveforms applied after those shown in Fig. 3. We note that the total charge passed, computed from the integral of the absolute value of the current, in experiments 4 and 5, in which no signif-

icant lesioning was observed, was comparable to that of experiment 3 (see Table 2 for details). The total charge passed did not appear to be the determining factor in lesioning.

**TABLE 2.** Charge passage statistics for each experiment calculated

Experiment	Maximum unbalanced charge $Q_{unbal}$ per cycle of periodic stimulus (mC)	Maximum unbalanced charge $Q_{unbal}$ during experiment (mC)	Unbalanced charge $Q_{unbal}$ at end of experiment (mC)	Total charge passed $Q_{pass}$ (mC)
1	1.0	9.7	-1.0	105
2	0.16	3.9	-3.9	105
3	15.0	57.5	-52.9	835
4	6.0	6.0	0.0	421
5	1.55	9.6	1.5	624
6	0.05	4.6	-2.9	32

Unbalanced charge,  $Q_{unbal}(T) = \int_0^T I(t) dt$ , computed by integrating the applied current. Maximum unbalanced charge computed as the largest absolute value  $Q_{unbal}$  during one stimulus period or full experiment. Unbalanced charge at end of experiment is computed from beginning to end of experiment. For most experiments, the periodic waveforms applied relatively low maximal charge variations. The majority of unbalanced charge came from nonperiodic stimuli applied after the experiments reported here. Total charge passed was computed by integrated absolute value of current,  $Q_{pass}(T) = \int_0^T |I(t)| dt$ . We attribute the severe lesioning observed in experiment 3 to the maximum unbalanced charge passed, and not the total charge passed.

## DISCUSSION

These experiments demonstrate that the use of radial electrical fields appears to be a feasible strategy for the modulation of epileptiform activity in the hippocampus. In several examples (experiments 5 and 6), modulation of ongoing activity was proportional to both the sign and amplitude of the applied field, with excitatory response observed in response to positive field and suppressive response observed in response to negative field.

The variability of the specific effects of positive or negative fields appeared related to the electrode placement with respect to the layers and geometry within the hippocampus. The two experiments (5 and 6) that best demonstrated modulation proportional to the stimulation amplitude and sign were those in which each electrode trajectory was confined to the central regions of the hippocampus. In these cases, we expect the electric field produced to be aligned with cell body layers, as shown in Fig. 2, over a significant length of hippocampus.

Such modulation with a radial field of alternating polarity is consistent with the classic work of Purpura and Malliani (37), in which surface polarization of the hippocampus increased and decreased hippocampal activity with opposite polarities, as required to modulate cortex (36). These results were consistent with the geometric inversion of the hippocampal pyramidal cells with respect to the ventricular surface compared with cortical pyramidal cells.

We observed bilateral modulation from unilateral stimulation (Fig. 4). Such observations suggest the possibility of modulating language-dominant hippocampi from non-dominant-side stimuli. A further speculation would be that bilateral temporal lobe seizures might be amenable to unilateral stimulation such as this.

Whether a pre-seizure state, defined by detectable dynamic changes from baseline before clear seizure onset, exists and what it may be is presently a topic of considerable interest for seizure prediction and control (48–50). We observed that perturbations associated with periodic field stimulation can demonstrate distinctive modulation of activity before a seizure (Fig. 4). That this modulation was observed far from the stimulus (contralateral) strongly suggests that the effect was not a measurement artifact from the stimulation. In addition, this modulation was not observed at any other time interictally except during the  $14 \pm 2$  s before seizures. Such a perturbation response could be quite useful in control-device design to probe for detecting dynamical changes just before an impending seizure. In addition, the normalized RMS deviation,  $\Delta$ , could be used to detect such modulation at very low stimulation amplitudes. Nevertheless, it remains to be shown how our observations from an acute seizure model translate to chronic spontaneous seizures in animals or human epilepsy.

The material used for our electrodes, Ag-AgCl, is unsuitable for human or long-term animal use. Fortunately, a number of nontoxic nonpolarizing electrode materials and manufacturing options are now available (51).

We observed acute lesioning in one experiment, which we attributed to extended application of DC (monopolar) current pulses that considerably polarized the stimulation electrode. Although the instantaneous current densities were low, the durations were large. We point this out specifically because lesion thresholds depend on both instantaneous current density and charge passage (see, for example, 52). Although there are considerable data on lesion thresholds for pulsatile stimulation (32,53,54), to our knowledge, no data exist on lesion thresholds from generation of continuous electric field and related currents from electrically nonpolarizing electrodes. The chronic lesion threshold will certainly be at lower charge passages than used here and depend on electrode material. A systematic exploration of the chronic lesion threshold for lesions at electrode surfaces for continuous waveforms with zero average charge transfer will be required before any attempt at human trials with prolonged continuous stimulation.

Our demonstration of hippocampal activity modulation with radial electric fields suggests that seizure control may be feasible with such stimulation. The next step is to develop and experimentally test control algorithms for modulation and feedback control of spontaneous seizures. The advantages of continuous electric field interaction with the hippocampus include the possibility of minimally invasive surgical strategies using percutaneous depth electrode insertion, in addition to subthreshold stimulation energies. Theoretically, because recording and stimulation can be made simultaneously and because the stimulation is both modulatory and graded with respect to the stimulation amplitude, it should be possible to minimize cognitive side effects. Lastly, whether a perturbation approach can serve as a useful strategy for definition and detection of a pre-seizure state is an intriguing possibility for future work.

**Acknowledgment:** This work was funded through a Biomedical Engineering Research Grant from the Whitaker Foundation RG990432, through National Institutes of Health grants K02MH01493, R01MH50006, NS020576, and training grant T32HD007459, and through the PACE foundation.

## REFERENCES

1. Cooper IS, Amin I, Riklan M, et al. Chronic cerebellar stimulation in epilepsy. *Arch Neurol* 1976;33:559–70.
2. Van Buren JM, Wood JH, Oakley J, et al. Preliminary evaluation of cerebellar stimulation by double-blind stimulation and biological criteria in the treatment of epilepsy. *J Neurosurg* 1978;48:407.
3. Velasco F, Velasco M, Velasco AL, et al. Effect of chronic electrical stimulation of the centromedian thalamic nuclei on various intractable seizure patterns, I: clinical seizures and paroxysmal EEG activity. *Epilepsia* 1993;34:1052–64.

4. Velasco F, Velasco M, Velasco AL, et al. Electrical stimulation of the centromedian thalamic nucleus in control of seizures: long-term studies. *Epilepsia* 1995;36:63–71.
5. Fisher RS, Uematsu S, Krauss GL, et al. Placebo-controlled pilot study of centromedian thalamic stimulation in treatment of intractable seizures. *Epilepsia* 1992;33:841–51.
6. Velasco F, Velasco M, Jimenez F, et al. Predictors in the treatment of difficult-to-control seizures by electrical stimulation of the centromedian thalamic nucleus. *Neurosurgery* 2000;47:295–304.
7. Benabid AL, Koussic A, Pollak P, et al. Future prospects of brain stimulation. *Neurol Res* 2000;22:237–46.
8. Benabid AL, Minotti L, Koussic A, et al. Antiepileptic effects of high-frequency stimulation of the subthalamic nucleus (corpus luyssi) in a case of medically intractable epilepsy caused by focal dysplasia: a 30-month follow-up: technical case report. *Neurosurgery* 2002;50:1385–92.
9. Loddenkemper T, Pan A, Neme S, et al. Deep brain stimulation in epilepsy. *J Clin Neurophysiol* 2001;18:514–32.
10. Hodaie M, Wennberg RA, Dostrovsky JO, et al. Chronic anterior thalamus stimulation for intractable epilepsy. *Epilepsia* 2002;43:603–8.
11. Mirski MA, Fisher RS. Electrical stimulation of the mammillary nuclei increases seizure threshold to pentylentetrazol in rats. *Epilepsia* 1994;35:1309–16.
12. Mirski MA, Rossell LA, Terry JB, et al. Anticonvulsant effect of anterior thalamic high frequency electrical stimulation in the rat. *Epilepsy Res* 1997;28:89–100.
13. McLachlan RS. Vagus nerve stimulation for intractable epilepsy: a review. *J Clin Neurophysiol* 1997;14:358–68.
14. Morris GL, Mueller WM. Long term treatment with vagus nerve stimulation in patients with refractory epilepsy. *Neurology* 1999;53:1731–5.
15. DeGiorgio CM, Schachter SC, Handforth A, et al. Prospective long-term study of vagus nerve stimulation for the treatment of refractory seizures. *Epilepsia* 2000;41:1195–200.
16. Sunderam S, Osorio I, Watkins JF III, Wilkinson SB, et al. Vagal and sciatic nerve stimulation have complex, time-dependent effects on chemically induced seizures: a controlled study. *Brain Res* 2001;918:60–6.
17. Fanselow EE, Reid AP, Nicoletis MA. Reduction of pentylentetrazole-induced seizure activity in awake rats by seizure-triggered trigeminal nerve stimulation. *J Neurosci* 2000;20:8160–8.
18. Patwardhan RV, Tubbs RS, Killingsworth C, et al. Ninth cranial nerve stimulation for epilepsy control, 1: efficacy in an animal model. *Pediatr Neurosurg* 2002;36:236–43.
19. Eder HG, Stein A, Fisher RS. Interictal and ictal activity in the rat cobalt/pilocarpine model of epilepsy decreased by local perfusion of diazepam. *Epilepsy Res* 1997;29:17–24.
20. Eder HG, Jones DB, Fisher RS. Local perfusion of diazepam attenuates interictal and ictal events in the bicuculline model of epilepsy in rats. *Epilepsia* 1997;38:516–21.
21. Yang XF, Rothman SM. Focal cooling rapidly terminates experimental neocortical seizures. *Ann Neurol* 2001;49:721–6.
22. Yang XF, Duffy DW, Morley RE, et al. Neocortical seizure termination by focal cooling: temperature dependence and automated seizure detection. *Epilepsia* 2002;43:240–5.
23. Bragdon AC, Kojima H, Wilson WA. Suppression of interictal bursting in hippocampus unleashes seizures in entorhinal cortex: a proepileptic effect of lowering  $[K^+]_o$  and raising  $[Ca^{2+}]_o$ . *Brain Res* 1992;590:128–35.
24. Barbarosie M, Avoli M. CA3-driven hippocampal-entorhinal loop controls rather than sustains in vitro limbic seizures. *J Neurosci* 1997;17:9308–14.
25. Jerger K, Schiff SJ. Periodic pacing an in vitro epileptic focus. *J Neurophysiol* 1995;73:876–9.
26. Weiss SR, Li XL, Rosen JB, et al. Quenching: inhibition of development and expression of amygdala kindled seizures with low frequency stimulation. *Neuroreport* 1995;6:2171–6.
27. Weiss SRB, Eidsath A, Li XL, et al. Quenching revisited: low level direct current inhibits amygdala-kindled seizures. *Exp Neurol* 1998;154:185–92.
28. Velasco AL, Velasco M, Velasco G, et al. Subacute and chronic electrical stimulation of the hippocampus on intractable temporal lobe seizure: preliminary report. *Arch Med Res* 2000;31:316–28.
29. Velasco M, Velasco G, Velasco AL, et al. Subacute electrical stimulation of the hippocampus blocks intractable temporal lobe seizures and paroxysmal EEG activities. *Epilepsia* 2000;41:158–69.
30. Lesser RP, Kim SH, Beyderman L, et al. Brief bursts of pulse stimulation terminate afterdischarges caused by cortical stimulation. *Neurology* 1999;53:2073–81.
31. Motamedi GK, Lesser RP, Miglioretti DL, et al. Optimizing parameters for terminating cortical afterdischarges with pulse stimulation. *Epilepsia* (in press).
32. Agnew WF, Yuen TGH, McCreery DB. Morphological changes after prolonged electrical stimulation of the cat's cortex at defined charge densities. *Exp Neurol* 1983;79:397–411.
33. Gordon B, Lesser RP, Rance NE, et al. Parameters for direct cortical electrical stimulation in the human: histopathological confirmation. *Electroencephalogr Clin Neurophysiol* 1990;75:371–7.
34. Bikson M, Lian J, Hahn PJ, et al. Suppression of epileptiform activity by high frequency sinusoidal fields in rat hippocampal slices. *J Physiol* 2001;531:181–91.
35. Denney D, Brookhart JM. The effects of applied polarization on evoked electro-cortical waves in the cat. *Electroencephalogr Clin Neurophysiol* 1962;14:885–97.
36. Purpura DP, McMurtry JG. Intracellular activities and evoked potential changes during polarization of motor cortex. *J Neurophysiol* 1965;28:166–85.
37. Purpura DP, Malliani A. Spike generation and propagation initiated in dendrites by transhippocampal polarization. *Brain Res* 1966;1:403–6.
38. Jefferys JGR. Influence of electric fields on the excitability of granule cells in guinea-pig hippocampal slices. *J Physiol* 1981;319:143–52.
39. Chan CY, Nicholson C. Modulation by applied electric fields of Purkinje and stellate cell activity in the isolated turtle cerebellum. *J Physiol* 1986;371:89–114.
40. Chan CY, Houndsgaard J, Nicholson C. Effects of electric fields on transmembrane potential and excitability of turtle cerebellar Purkinje cells in vitro. *J Physiol* 1988;402:751–71.
41. Tranchina D, Nicholson C. A model for the polarization on neurons by extrinsically applied electric fields. *Biophys J* 1986;50:1139–59.
42. Gluckman BJ, Neel EJ, Netoff TI, et al. Electric field suppression of epileptiform activity in hippocampal slices. *J Neurophysiol* 1996;76:4202–5.
43. Ghai RS, Bikson M, Durand DM. Effects of applied electric fields on low-calcium epileptiform activity in the CA1 region of rat hippocampal slices. *J Neurophysiol* 2000;84:274–80.
44. Gluckman BJ, Nguyen H, Weinstein SL, et al. Adaptive electric field suppression of epileptic seizures. *J Neurosci* 2001;21:590–600.
45. Traub RD, Miles R. *Neuronal networks of the hippocampus*. Cambridge: Cambridge University Press, 1991.
46. Paxinos G, Watson C. *The rat brain in stereotaxic coordinates*. 3rd ed. San Diego: Academic Press, 1997.
47. Fisher AC. *Electrode dynamics*. Oxford: Oxford University Press, 1996.
48. Le Van Quyen M, Martinerie J, Navarro V, et al. Characterizing neurodynamic changes before seizures. *J Clin Neurophysiol* 2001;18:191–209.
49. Lehnertz K, Andrezejak RG, Arnhold J, et al. Nonlinear EEG analysis in epilepsy: its possible use for interictal focus localization, seizure anticipation and prevention. *J Clin Neurophysiol* 2001;18:209–23.
50. Litt B, Esteller R, Echaz J, et al. Epileptic seizures may begin hours in advance of clinical onset: a report of five patients. *Neuron* 2001;30:51–64.
51. Meyer RD, Cogan SF, Nguyen TH, et al. Electrodeposited iridium oxide for neural stimulation and recording electrodes. *IEEE Trans Neural Syst Rehabil Eng* 2001;9:2–11.
52. Weiland JD, Anderson DJ. Chronic neural stimulation with thin-film, iridium oxide electrodes. *IEEE Trans BME* 2000;47:911–8.
53. Babb TL, Soper HV, Lieb JP, et al. Electrophysiological studies of long term electrical stimulation of the cerebellum in monkeys. *J Neurosurg* 1977;47:353–65.
54. Gordon B, Lesser RP, Rance NE, et al. Parameters for direct cortical electrical stimulation in the human: histopathologic confirmation. *Electroencephalogr Clin Neurophysiol* 1990;75:371–7.